Journal of Materials Chemistry A

Accepted Manuscript

ROYAL SOCIETY OF CHEMISTRY

www.rsc.org/materialsA

Journal Name

ARTICLE

Facile preparation of a mechanically robust superhydrophobic acrylic polyurethane coating

Received 00th January 20xx,
Accepted 00th January 20xx

DOI: 10.1039/x0xx00000x

www.rsc.org/

Fang Xue, Dongmei Jia, Yu Li*and Xinli Jing

Superhydrophobic (SH) surface is usually constituted by a combination of low surface energy substances and micro- and nanometer scale roughness structures. The latter, however, always have poor mechanical strength and requires complicated fabrication procedures, seriously hindering the large-scale preparation and industrial application of SH surfaces. In this study, by introducing fluoroalkyl silanes modified silica nanoparticles into hydroxyl acrylic resin and using a simple spray-coating method, an SH acrylic polyurethane (SAPU) coating with good abrasion resistance and stable adhesion was obtained after cross-linking with polyisocyanate at room temperature. By virtue of the reaction between silanol groups in silica NPs and isocyanate groups in the curing agent, the hydrophobic silica NPs were stably anchored into the SAPU resin matrix while constructing hierarchical micro- and nanometer scale roughness structures on the coating surface. The dual characters ensure the SAPU coating has a static water contact angle (CA) of >160°, a sliding angle of ~ 10° and good mechanical property, which exhibits CAs of >150° after weraing with a sandpaper and keeps a strong adhesion even after cross-cutting or impacting tests. Moreover, the SAPU coating retains an excellent water-repellent property after a 12 h immersion in hydrocholoric acid with pH=1, and can recover its water-repellent property after 12 h immersion in sodium hydroxide solution with pH=14 through hot air blowing. The facile spray-coating method as well as a mild room temperature curing process make this kind of SH coating especially suitable for non-wetting protection or modification of large-scale parts, providing a novel pathway to the development of a high performance SH surface.

1 Introduction

Bearing both a high water contact angle (>150°) and a low water roll-off angle (<10°), a superhydrophobic (SH) layer offers a quick roll-off performance of a water droplet from its surface, which is very attractive in application fields such as self-cleaning, non-wetting, anti-fogging and anti-icing.[1-5] Besides components with low surface energy, micro- and nanometer scale roughness structure is expected to provide a high CA and a low CA hysteresis, since this kind of structure can hold air in its gaps thus decreasing the contact area between a droplet and the surface. Therefore, the construction of micro- and nanometer scale roughness structures is very important to develop SH surfaces.[6-9] A myriad of methods have been reported to fabricate micro- and nanometer scale roughness structures, for example, combination of polymers with inorganic nanoparticles,[10] template synthesis,[11] phase separation method,[12] casting method,[13] chemical etching and mechanical treatment.[14]

However, the micro- and nanometer scale roughness structures are usually very fragile, which can be easily destroyed or removed by mechanical abrasion, water impact or even finger touching, leading to a drastic decrease of CA and loss of superhydrophobic property.[7, 15] Moreover, the construction of SH layers usually requires components with low surface energy such as fluorine or silica containing substances, which always have poor adhesion to lots of substrates. Therefore, it is rather a challenge to obtain surfaces with both an excellent water roll-off property and a long-life mechanical durability [15, 16]. The mechanical durability has become a bottleneck which seriously restricts the industrial application of SH surfaces,[17] and many efforts have been made to conquer this shortcoming. One solution is creating robust micro- and nanometer roughness structures which are comprised of metal NPs or have strong bonding to the substrate, in comparison with fragile micro- and nanometer scale roughness structures created by sol-gel method[18], phase separation, crystal growth[7] or electrostatic deposition[19]. The methods for robust roughness structures include micro and nano mechanical manufacturing[20, 21], sandblasting[22], chemical vapour deposition[19], etching[23], plasma treatment or assisting with film-forming polymers,[24] etc. Another effort is to improve the abrasion resistance of the components forming the SH surface or to protect the fragile roughness structures by sacrificial components. For instance,

Department of Applied Chemistry, School of Science, Xi'an Jiaotong University, Xi'an, 710049, People's Republic of China. E-mail: yuli2012@mail.xjtu.edu.cn, rgfp-jing@mail.xjtu.edu.cn

Electronic Supplementary Information (ESI) available: [details of any supplementary information available should be included here]. See DOI: 10.1039/x0xx00000x

Su et al. prepared an SH surface with excellent abrasion resistance by casting a polyurethane precursor on a porous aluminium template.[25] Zhou et al used polydimethylsioxane (PDMS) filled with fluorinated alkyl silane functionalized silica NPs producing an SH coating on fabrics which can endure severe abrasion damages and exposure to boiling water[26]. By using large scale micropillars to protect the fine-scale surface patterns, Huovine et al. developed an excellent mechanically robust SH surface which can maintain its non-wetting property in a mechanical compression up to 20 MPa and in an abrasive-wear test up to 120 kPa[20].

In recent years, development of layers with self-healing or easy repairability functions has become a new trend to prolong the lifespan of SH layers. An important approach is to encapsulate the hydrophobic component in the pores of the rough nanoporous materials, as reported by Sun et al.,[27] which can release healing agents to restore the SH performance in case of mechanical damage. By spraying polystyrene/silica core-shell nanoparticles as a coating skeleton and PDMS as a hydrophobic interconnection, Xue et al.[28] fabricated a lasting and self-healing superhydrophobic surface, which exhibits durability by automatically restoring the damage through room temperature or heat curing and tetrahydrofuran treatment. Reorganization of colloidal particles at the interface is another method to endow a self-healing function to the SH surface, as reported by Puretskiy et al, the migration of colloidal particles due to melting of wax induced restoration of the SH behaviour. [29] Zhu et al.[30] prepared a superhydrophobic surface based on metal/polymer composite to achieve both mechanical durability and easy repairability. The non-wetting property of this surface can be restored by an easy regeneration process i.e. repeating the Ag deposition and surface fluorination.

In our opinion, an SH layer with high mechanical strength should meet at least two requirements, ① stable adhesion of the layer to its substrate and ② strong bonding of micro- and nanometer scale roughness structures to the layer matrix. By virtue of the good film-forming performance of resins and hard inorganic NPs with easily modified surface property and facilely adjustable sizes, it has been an effective way to fabricate SH layers or surfaces by introducing inorganic NPs into the resin matrix to construct micro- and nanometer scale roughness structures.[10, 16, 28, 31, 32] In past research, epoxy resin[24, 33] and polymethyl methacrylate[16] have been widely used to strengthen the adhesion of NPs. Besides that, bi-component acrylic polyurethane is very attractive due to its remarkable advantages such as excellent abrasive resistance, good flexibility and high adhesion to many kinds of substrates, which can probably compensate the poor mechanical properties of ordinary SH layers. Silica NPs, which are easy to prepare, with diameters facilely controlled and rich Si-OH groups suitable for modification, have been widely introduced into resin matrix as hydrophobic fillers to fabricate SH surfaces.[34-36] Recently, Ramakrishna et al. reported the preparation of a kind of SH coating using oligomer wrapped silica NPs obtained through reactions between silanol and isocyanate groups[35]. Based on appropriate grafting to the silica NPs, fluorine or silane chemistry was not required in this kind of SH coating which still showed excellent non-wetting property and good tolerance to pH and mechanical damages. Nevertheless, it is often difficult to acquire a strong bonding of inorganic NPs to the resin matrix while maintaining a sufficient roughness structure to hold the SH property. When the NPs are completely buried in the resin matrix, the mechanical strength of the layer will be undoubtedly good without constituting any roughness structure. If the NPs are just slightly adhered to or sputtered on the layer surface, the roughness structure will be obtained and can be easily damaged or removed under mechanical abrasion.

In this study, hydrophobically modified silica NPs with facilely tuned sizes and reactive silanol groups were introduced into bi-component acrylic polyurethane resin. By spraying this organic-inorganic mixture and curing it at room temperature, an SH coating with both an outstanding non-wetting property and excellent mechanical properties was obtained, based on the micro- and nanometer scale roughness structures constructed by hydrophobic silica NPs and their interaction with the resin matrix. This kind of SH coating constructed with a facile method is supposed to have great potential uses in industrial applications requiring a lotus-effect and high mechanical performance.

2. Experimental

2.1 Materials

(Heptadecafluoro-1,1,2,2-tetrahydrodecyl)trimethoxysilane ($CF_3(CF_2)_7CH_2CH_2Si(OCH_3)_3$, FAS-17) was purchased from SICONG Chemical(Quanzhou, China), hydroxy acrylic resin which is a random copolymers of acrylate monomers (Scheme S1, with a hydroxyl content of 3.4 wt%, a solid content of 70wt%) and butyl acetate (BA) were provided by Zhejiang Desoul Chemical Technology Co., Ltd. (Deqing, China). The curing agent was a trimer of hexamethylene diisocyanate (HDI) purchased as Bayer product N3390 (90wt%). Tetraethyl orthosilicate ($Si(OCH_2CH_3)_4$, TEOS), ethanol and aqueous ammonium (25 wt%) in analytical purity were provided by Tianjin Kemiou Chemical Reagent Co., Ltd. (Tianjin, China). All the chemicals were used as received.

2.2 Preparation and functionalization of silica NPs

In this general sol-gel procedure, 50 g of ethanol and 10 g of aqueous ammonia are evenly mixed at room temperature, into which 10 g of TEOS is added. The mixture (with pH=11-12) is put into a water bath of 50 ℃ and mechanically stirred. After 0.5 h of stirring, 1 g of FAS-17 is added into the reaction mixture and the mixture is stirred for another 2 h. Then, the obtained mixture is vacuum filtrated with a Buchner funnel and the filtrate cake is dried under vacuum (50 ℃) to give the functionalized silica NPs (F-silica NPs).

2.3 Preparation of SAPU and APU coatings

Dissolve 3 g of hydroxyl acrylic resin into 15 g of BA to make a homogeneous dilute resin solution. Add 2 g of F-silica NPs into the resin solution and treat the mixture under ultrosonic wave or high-speed dispersing to make it evenly (noted as part A). Weigh a certain amount of N3390 (*ca.* 1.2 g) as part B based on the molar ratio of isocyanate groups to that of hydroxyl groups in part A of 1.1:1. Then mix part A and part B evenly and spray or drop-wise coat the mixture onto glass substrate or polished iron (tinplate) sheets. After curing at room temperature for 12 h or curing at 80℃ for 30 min, an SAPU coating with good mechanical property was prepared. The synthetic procedure of the SAPU coating was shown as Scheme S2 (SI).

2.4 Characterization

2.4.1 Morphology

Morphologies of silica NPs and F-silica NPs were observed with a JEM-2100 transmission electron microscopy (TEM) in an acceleration voltage of 200 kV. For TEM examination, the silica NPs were dispersed in ethanol with ultrasonic treatment for 0.5 h to form suspensions with concentrations of *ca.* 0.05 gml^{-1}. Surface morphologies of the coatings made of F-silica, APU and SAPU were characterized by the scanning electron microscope (SEM, JSM-6700F, JEOL) after gold-sputtering. Root-mean-square (RMS) roughness values of the APU coating and SAPU coating were characterized on a Dimension Icon atom force microscope (AFM, Bruker) in a tapping mode.

2.4.2 Structure

FTIR spectra of the samples were recorded between 4000 cm^{-1} and 400 cm^{-1} on a Bruker Tensor-27 spectrophotometer. FTIR spectrum of APU coating was recorded in a reflection mode since the layer is too flexible to be grounded into powder. A little amount of SAPU coating as well as the reaction products of N3390 and F-silica was scratched off and grounded with KBr to press pellets for recording their FTIR spectra in a transmission mode. Surface elemental compositions of the casting films were investigated by X-ray photoelectron spectra (XPS) using a Thermo Scientific K-Alpha X-ray photoelectron spectrometer with an AlK_{α} source.

2.4.3 Contact angle and slide angle

Static water contact angle (CA) and water slide angle (SA) were measured with 5-8 μL of water (larger volume of water droplet was used when the surface was too hydrophobic) using an optical contact angle meter (Attention Theta). SA measurements were determined by slowly tilting the sample stage until the water droplets started moving. Each of the reported CAs and SAs represents the average value of five measurements.

2.4.4 Mechanical properties

The abrasion resistance test was carried out by using 2000 mesh sandpaper with 100 g of loading (corresponding to a force of *ca.* 2 kPa) onto the SAPU surface and APU surface coated on glass slides (25.4 mm×76.2 mm) and moving the sandpaper from one side to another parallel to the coating surface at *ca.* 21 cm s^{-1} . A moving cycle from back to forth was calculated as a one time abrasion. Weight loss, surface morphology and CA of SAPU coating after different times (50, 100, 150, 200) of wearing were recorded to evaluate its abrasion resistance in comparison with the APU coating.

According to the standardized coating adhesion test method (GB9286-88), cross-cutting tests were carried out by scratching the SAPU coating into 1×1 mm grids with a cut-off knife and tearing off with a 3M 610 tape to check its adhesion to the substrate.

The mechanical property of the SAPU coating was further evaluated through the falling hammer impact test according to the standard (GB/T 1732-1993). The maximum height of a 1 kg hammer vertically dropped, without causing damage to the coating, was recorded.

3 Results and discussion

3.1 Hydrophobic F-silica NPs

Silica NP_S with diameters around 100 nm formed after 0.5 h hydrolysis of TEOS in alkaline medium. It was shown that these NPs aggregated into small clusters of ca. 300 nm even after 0.5 -1 h of sonication treatment in ethanol, indicating their micro- and nanometer scale multiple structures. After another 2 h hydrolysis of TEOS in the presence of FAS-17, the morphology and size of the major products did not change a lot, whereas much smaller clusters composed of NPs with diameters of several tens of nanometer appeared, which can be attributed to hydrolysis products of FAS-17.

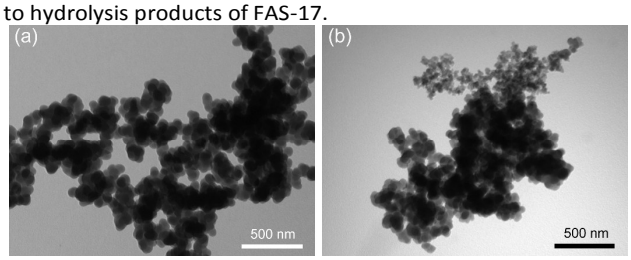

Figure 1. Typical TEM images of silica NPs obtained after 0.5 h hydrolysis of TEOS (a) and F-silica NPs obtained after another 2 h hydrolysis in the presence of FAS-17.

FTIR spectra showed that fluorine has been successfully incorporated into F-silica NPs, which still retain a lot of hydroxyl groups adaptable for subsequent reaction. As shown in Figure 2, F-silica NPs display FTIR spectrum similar to that of silica NPs, in which intense peaks belonging to the Si-O-Si[37] structure and silanol groups can be clearly observed at 1099 cm^{-1} and 3446 cm^{-1} respectively. In the spectra of F-silica, additional peaks at 1209 cm^{-1} and 1150 cm^{-1} apppeared, which embody the vibration of the C-F structure in the fluorinated alkyl chains.[38] The peaks at 706 and 656 cm^{-1} can also be attributed to a combination of rocking and wagging stretchings of CF_2 structures.[39]

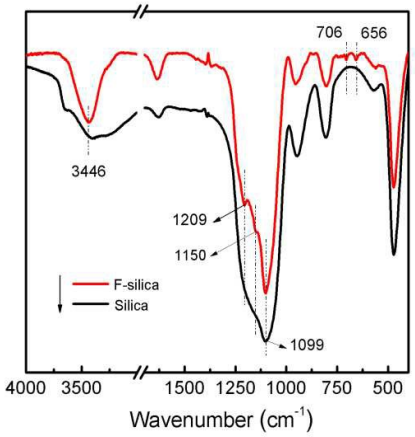

Figure 2. FTIR spectra of silica NPs and F-silica NPs.

Benefiting from their micro- and nanometer scale multiple structures and low surface energy fluoroalkyl groups, F-silica NPs exhibit excellent superhydrophoic property with a CA high to 165°. By casting the dispersion of F-silica NPs onto a glass slide and drying it in air, a white layer is formed which can repel water droplets quickly. SEM examination showed that F-silica NPs on the surface of this layer aggregated into clusters with edge sizes of 1-2 μm, leaving lots of micro-mater scale cavities to hold air. The CA of the F-silica layer is around 165°, which is distinctly different from the layer composed of silica NPs, i.e., the latter is highly hydrophilic and can even absorb the water droplets quickly. This performance again confirmed that fluoroalkyl groups have been successfully incorporated into the F-silica products, which in combination with the micro- and nanometer scale roughness structure contributes to the SH property. The as-prepared F-silica NPs, even without removing un-reacted FAS-17, were found to be stable under the enviroment condition and can maintain their SH property for up to one year, avoiding the use of large amount of organic solvents in case of large scale production.

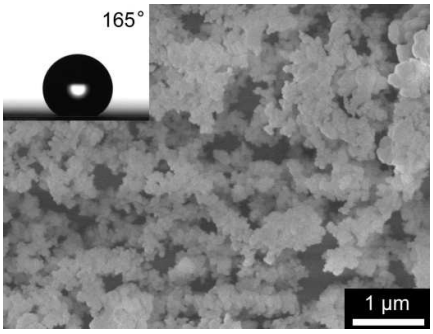

Figure 3. A typical SEM image of surface made of F-silica NPs, the inset is a snapshot of the measured CA.

3.2 SAPU coating containing F-silica NPs

By virtue of the interaction between silanol groups in F-silica NPs and isocyanate groups of the curing agent, F-silica NPs were stably anchored into the cured APU resin matrix. In a typical preparation procedure for the mechanical robust SAPU coating, F-silica NPs were first mechanically mixed with a diluted hydroxyl acrylic resin solution of a solid content around 14%, into which a certain amount of curing agent N3390 was added. Bearing nanometer scale small sizes and a certain amount of un-reacted silanol groups, F-silica NPs can be easily mixed with the dilute solution of acrylic resin in butyl acetate to form a milky white dispersion (Supplementary information, SI, Figure S1) through high-speed dispersing or treated with ultrasonic irradiation for ca. 1 h. When this dispersion was mixed with a curing agent and sprayed (or casted) onto an tinplate (or glass substrate), it turned out to be semi-transparent. This semi-transparent film gradually became white and non-transparent as the curing process proceeded, whereas the APU coating without silica NPs prepared at the same condition maintained a semi-transparent state. This can be explained as partial phase separation may probably occur during the curing of SAPU coating, in which the F-silica NPs with low surface energy tend to gather to the top surface as the solvent evaporates. The coatings of SAPU and APU were cured at room temperature for 12 h. As control, F-silica NPs were mixed with N3390 at the same weight ratio as that used for SAPU coating and the mixture was left for reaction at the same conditions as the curing. The three kinds of products were then analyzed using FTIR.

As shown in Figure 4, the FTIR spectrum of APU coating displays typical peaks belonging to acrylic resin cured with isocyanate, e.g., the peak at 1150 cm^{-1} represents a C-O structure in aliphatic ester; the peaks at 2844 cm^{-1} and 2937 cm^{-1} are attributed to the symmetric and asymmetric stretching vibrations of C-H in CH_2 group, respectively. The peak at 1691 cm^{-1} indicates the C=O structure in the amino ester -O-C(O)-NH- unit due to the reaction between hydroxyl groups of acrylic resin and isoyanate groups in N3390.[35] In comparison with APU coating, an intense peak belonging to the C=O structure is also clearly shown and an additional peak corresponding to stretching vibration of Si-O appeared in the FTIR spectra of SAPU coating, confirming the presence of F-silica NPs. Similarly, the FTIR spectrum of the processed mixture of F-silica and N3390 displays the peak belonging to the C=O bond in the -O-C(O)-NH- unit at the same position as that of SAPU and APU, besides an intense peak due to the presence of Si-O-Si structure, indicating that the reaction between silanol groups and isocyanate groups has taken place at the curing condition (Scheme 1). A schematic structure illustrating the bonding between N3390 and F-silica was given in Scheme 1. In the FTIR spectrum of reaction product of F-silica and N3390, a small peak corresponding to the –NCO structure can still be observed, since no acrylic resin was used in this case, the silanol groups in F-silica are insufficient to consume all the isocyanates in N3390.

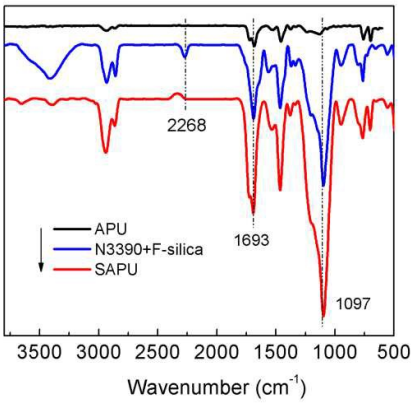

Figure 4. FTIR spectra of APU、SAPU coatings and the reaction product of N3390 and F-silica obtained at the same curing condition.

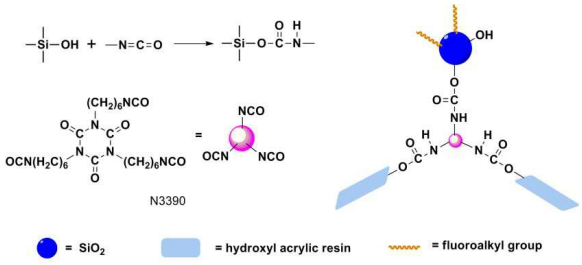

Scheme 1. Reaction between the silanol group and the isocyanate group[35] and the possible bonding structure between the resin matrix and F-Silica NPs through N3390.

XPS analysis further confirmed that the top surface of SAPU coating is rich in fluorine and silicon, which provides the materials base for the SAPU coating's SH performance due to their low surface energy. As shown in Table 1, in comparison with the APU coating prepared at the same curing condition, a significant content of fluorine and silicon was detected in the surface of the SAPU coating. The fluorine content in the SAPU surface is close to that in pure FAS-17 on the same substrate, whereas the silicon content is even higher than that in FAS-17, indicating the surface of SAPU coating is mainly composed of F-silica NPs.

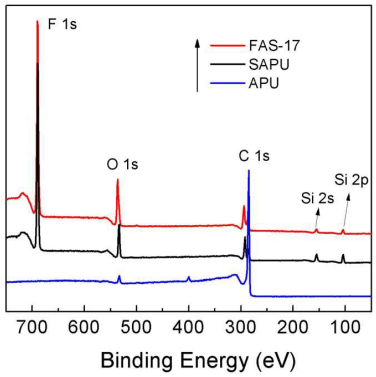

Figure 5. XPS spectra of an APU coating, SAPU coating and FAS-17 on a glass substrate.

Table 1. XPS elemental analysis of an APU coating, an SAPU coating and FAS-17 (at.%)

Sample	C	F	O	Si	N
APU	94.2	/	2.96	/	2.82
SAPU	31.31	47.81	12.42	8.46	/
FAS-17	32.35	46.35	17.15	4.16	/

F-silica NPs with low surface energy constructed micro- and nanometer scale roughness structures with lots of cavities on the surface of SAPU coating after curing, gave excellent SH performance. Water droplets dripped on this SAPU coating maintained a nearly spherical shape and can easily roll off (SI, video 1), whereas water droplets of the same volume on the APU coating tended to stick to the surface and displayed a spherical crown shape (Figure 6). SEM examination showed that 3-6 μm aggregates constituted by NPs with diameters of 70-400 nm formed on the surface of SAPU coating, which is similar to the texture structures of the surface merely composed of F-silica NPs. As a comparison, the surface of APU coating is smooth and even, with few cavities observed(Figure 6, a). We noticed that the surface structure became more rough when the content of F-silica NPs was increased (SI, Figure S2). AFM images further confirmed the multiple micro- and nanometer scale roughness structure of SAPU, which showed micrometer scale aggregates created by nearly spherical nanoparticles. With an F-silica NPs content of 39% corresponding to the solid weight of the coating, the SAPU surface showed RMS roughness of 135 nm, which is significantly higher than that of its counterpart; the APU coating of just 2.08 nm (Figure 7). At this condition, the unique roughness structure as well as the fluorine containing components contribute a significant increase of CA from 84° for the pristine APU coating to 162° for the SAPU coating (Figure 6). The specific roughness strucutre as well as low surface energy component on the SAPU coating also ensures its excellent oleophobic property, e.g., a CA high to 142° for n-hexadecane was obtaiend(SI, Figure S3).

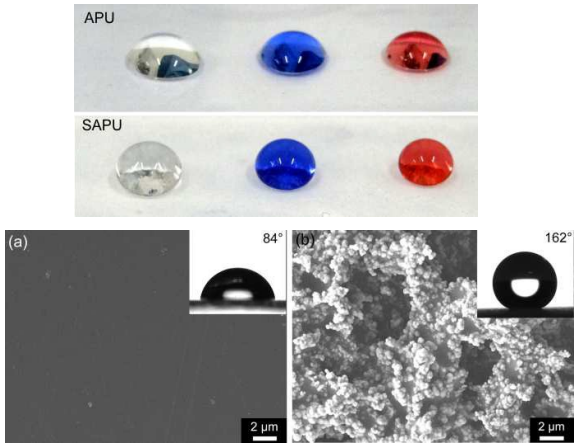

Figure 6. Optical images (top) of water drops (all in *ca.* 40 µL, the blue and red water drops were coloured with ink) on the APU and SAPU coatings and typical SEM images of APU surface (a) and SAPU surface (b), the insets are their CAs.

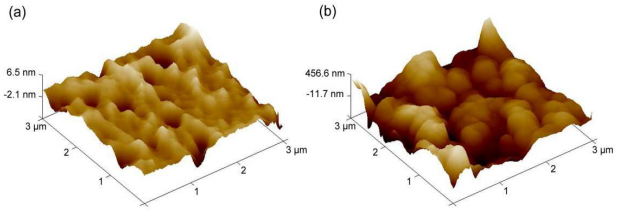

Figure 7. AFM images of the surfaces of an APU (a) coating and an SAPU coating (b).

An appropriate hydrolysis procedure of FAS-17 during the preparation of F-silica NPs as well as its content is particularly required to obtain SAPU coating with high CA and low SA. For instance, we found that if the hydrolysis time of FAS-17 was too long or too short i.e., FAS-17 was fed with TEOS at the beginning of the sol-gel process or fed 2 h after the hydrolysis of TEOS, the resulted F-silica NPs did not provide a good SH property. It can be explained by silica NPs not being effectively modified with FAS-17, since FAS-17 can hydrolyze to form NPs by themselves (in the former case) or not having enough time to react with pre-formed silica NPs (in the latter case). Furthermore, at least 30% of the weight content of F-silica NPs corresponding to the total weight of the coating is required to obtain SAPU coating with a CA higher than 150°. Otherwise, the NPs can be easily buried in the viscous resin matrix and thus can not form effective roughness structure after curing. Meanwhile, in order to enable a good mechanical performance besides the SH property, the maximum content of F-silica in the coating should not be higher than 50 wt%.

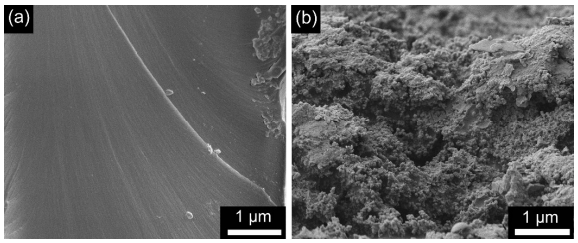

Figure 8. Typical SEM images of the cross section of an APU coating (a) and a SAPU coating (b, with F-silica NPs content of 39%).

SEM examinations on the cross-section of an APU coating and a SAPU coating showed that the latter displayed an evident rough structure in a *ca.* 5-6 µm thickness range from the layer top surface (Figure 8). Moreover, it was noticed that nearly in the whole thickness range of the layer is full of F-silica NPs (SI, Figure S4). This structural character indicates the durable feature of the SAPU coating [40] i.e., the surface is probably hydrophobic in bulk, which will probably retain the SH performance even when the top layer roughness is destroyed.

Considering the synthetic process of the SAPU coating, it does not need multiple procedures to produce hierarchical structures or to protect surface roughness [20, 41]. And it is different from methods which use micro and nano manufacturing procedures[21] to plant or deposit nanoparticles[30, 42] in order to construct robust roughness structure. Moreover, the raw materials used are commercially available and cheap, and special or expensive post-treatment procedures are not required. It will be easy to prepare this kind of SH coating on a large scale with sparying technique suitable for painting of large parts, so the SAPU coating will be very attractive for industrial application.

3.3 Mechanical property and pH-tolerant

Due to the hardness of F-silica NPs and their stable bonding to the acrylic resin matrix, the SAPU coating suffers a lower weight loss as compared to the APU coating under the same abrasion conditions, and retains a CA higher than 150° even after 200 abrasions with sandpaper. After curing, the SAPU coating is very sturdy and durable, and showed almost no damage after water injecting or finger touching. In order to evaluate its abrasion resistance, the cured SAPU coating and APU coating on glass slides were abrased using a 2000 mesh sandpaper with *ca.* 2kPa force from one side to another. After a certain number of abrasion cycles, the weight loss of the SAPU coating was found even to be smaller than that of APU (SI, Table 1). This can be explained as F-silica NPs which served as hard fillers dissipate the abrasion energy thus improve the abrasion resistance of pristine APU coating. Nevertheless, it can be seen that after 50 abrasions, when the NPs as well as their aggregates protruded onto the SAPU surface were firstly removed, the surface became smoother with fewer cavities (Figure 9, b) and its CA decreased from 162° to 159°. As the number of abrasion cycles increased, a portion of the micrometer scale roughness structure was destroyed, CA of the SAPU coatings decreased a little, whereas the SA increased significantly(Figure 10). It seems that an SAPU coating after 200 abrasions is still rougher than an unpolished APU coating (Figure 6, a). The drastically increased SA indicates that multiple micro- and nanometer scale roughness strucutres contribute a lot to lowering the SA of the surface. An interesting phenomenon was noticed that after 150 abrasions, the CA of the SAPU coating was slightly increased to 157°(Figure 10), whereas its SA was also increased. The slightly increased CA can be attributed to new roughness structures created by sandpaper wearing during abrasion.

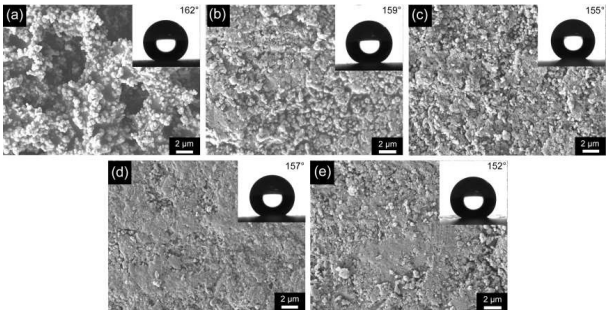

Figure 9. SEM images of an original SAPU coating surface (a), the surface of SAPU coating after 50 (b), 100 (c), 150 (d) and 200 (e) cycles of abrasion, the insets are the corresponding CAs of these surfaces.

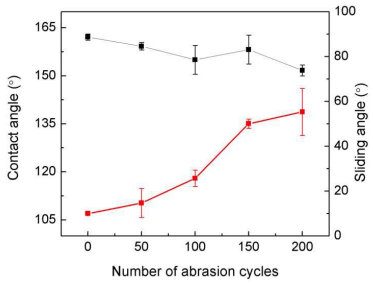

Figure 10. CAs and SAs of the SAPU coating after a certain number of abrasion cycles.

The SAPU coating retains the excellent film-forming properties of bi-component acrylic polyurethane resin, which shows high adhesion to substrates such as glass and tinplate, and displays good resistance to impact. After curing, the SAPU coating sprayed onto a tinplate can even be scratched with a cut-off knife without coming off of silica powders or film fragments, indicating again the strong bonding of F-silica to the resin matrix. The scratched SAPU coating showed grids with clear and neat edges, which did not induce any exfoliation even by peeling off with a 3M 610 tape. According to the coating adhesion test standard, it can be said that this kind of SAPU coating possesses a high level of adhesion which meets the application requirement in this field. Moreover, it was shown that the scratching even did not induce significant change of the surface morphology (SI, Figure S5).

The mechanical property of the SAPU was further characterized through the impact test. In this case, a 1 kg weight hammer was released to fall free from a 50 cm height onto a tinplate coated with SAPU coating. After the fall a dent was formed on the tinplate whereas the SAPU coating was undamaged, i.e. no cracking and exfoliation were observed with the naked eye and the surface morphlogy of the coating was scarcely destroyed (SI, Figure S6), no matter if the impact was on the front or back of the tinplate. Therefore, the impact resistance is also qualified to the requirements for organic coatings. Furthermore, it is interesting to notice that, when a water droplet was put on the upper edge of an impact dent, it quickly repelled off or rolled off to the bottom center of the dent (SI, video 2), further indicating the excellent SH performance even after impacting.

It is interesting to find that the SAPU coating obtained in our work maintains or recovers the SH property even after strong acidic or basic solution treatment. Two SAPU coatings on glass slides were immersed into hydrochloric acid with pH=1 and the sodium hydroxide solution with pH=14, respectively. After 12 h of immersion, the surface of SAPU coating treated with hydrocholoric acid did not show any change and seemed to be as dry as before immersion without even tiny water spots (SI, Figure S7). By stripping a water drop to the SAPU surface just taken out form the hydrocholoric acid solution, the water drop still maintained a near spherical shape and can easily roll off even by slightly shaking the substrate horizontally (SI, video 3), indicating that the SAPU coating with SH property has a strong tolerance to highly acidic solution. It was also noticed that the non-wetting property of the SAPU coating was partially reduced after *ca.* 4 h and totally gone after 12 h immersion in the sodium hydroxide solution with pH=14 (SI, video 4). This may be due to the affinity of silica NPs to the sodium hydroxide solution, leading to a diffusion of water molecules into the air pockets on the SAPU surface. Fortunately, when the surface immersed in the sodium hydroxide solution was dried, using a hot blower for *ca.* 2 min, a water drop dripped onto it rolled off easily again (SI, video 5), indicating its SH property had been recovered.

4. Conclusions

In this work, we have shown that a mechanically robust SH coating with good chemical resistance was facilely prepared based on bi-component acrylic resin and fluoroalkyl silane modified silica NPs. The excellent film-forming property of acrylic resin and low surface energy, micro-and nanometer scale roughness provided by F-silica NPs were effectively combined through the reaction between surface hydroxyl groups on F-silica NPs and isocyanate groups. As a result, the as-prepared SAPU coating displayed a water CA higher than 162° and a SA lower than 10°, which can retain a CA higher than 150° after 200 cycles of abrasion using a sandpaper with ca. 2 kPa force. The SAPU coating maintained undamaged even under hammer impacting or cross-cutting, indicating its high mechanical strength. Moreover, after immersion in acidic solution (pH=1) for 12 h, the SAPU coating still showed an excellent water-repellency property and after immersion in a strong basic solution (pH=14) this performance was recovered through hot air blowing. In comparison with SH layers reported in the literature, it is easy to prepare the SAPU coating on a large scale, this will be very attractive for development of high-performance surfaces for self-cleaning, anti-icing and anti-fouling, etc. suitable for industrial use.

Acknowledgements

The authors highly appreciate financial supports from Zhejiang Desoul Chemical Technology Co., Ltd. and the Fundamental Research Funds for the Central Universities (No. XJJ 2014008) for this work.

Notes and references

1 H. Y. Erbil, A. L. Demirel, Y. Avcı and O. Mert, *Science*, 2003, **299**, 1377-1380.
2 S. Farhadi, M. Farzaneh and S. A. Kulinich, *Appl. Surf. Sci.*, 2011, **257**, 6264-6269.
3 J. Zimmermann, F. A. Reifler, G. Fortunato, L. C. Gerhardt and S. Seeger, *Adv. Funct. Mater.*, 2008, **18**, 3662-3669.
4 R. Menini and M. Farzaneh, *J. Adhes. Sci. Technol.*, 2011, **25**, 971-992.
5 M. He, J. Wang, H. Li and Y. Song, *Soft Matter*, 2011, **7**, 3993-4000.
6 Z. Xi, S. Feng, N. Jia, J. Yugui and W. Zhiqiang, *J. Mater. Chem.*, 2008, **18**, 621-633.
7 P. Roach, N. J. Shirtcliffe and M. I. Newton, *Soft Matter*, 2008, **4**, 224-240.
8 D. Öner and T. J. McCarthy, *Langmuir*, 2000, **16**, 7777-7782.
9 L. Gao and T. J. McCarthy, *Langmuir*, 2006, **22**, 2966-2967.
10 S. Rezaei, I. Manoucheri, R. Moradian and B. Pourabbas, *Chem. Eng. J.*, 2014, **252**, 11-16.
11 J. Y. Cheng, C. Ross, E. L. Thomas, H. I. Smith and G. J. Vancso, *Adv. Mater.*, 2003, **15**, 1599-1602.
12 Q. Xie, J. Xu, L. Feng, L. Jiang, W. Tang, X. Luo and C. C. Han, *Adv. Mater.*, 2004, **16**, 302-305.
13 X. Du and J. He, *Acs Appl. Mater. Inter.*, 2011, **3**, 1269-1276.
14 J. T. Han, X. Xu and K. Cho, *Langmuir*, 2005, **21**, 6662-6665.
15 N. J. Shirtcliffe, G. McHale and M. I Newton, *J. Polym. Sci. Part B: Polym.Phys.*, 2011, **49**, 1203-1217.
16 S. S. Latthe, C. Terashima, K. Nakata, M. Sakai and A. Fujishima, *J. Mater. Chem. A*, 2014, **2**, 5548-5553.
17 M. Callies and D. Quéré, *Soft Matter*, 2005, **1**, 55-61.
18 B. P. Dyett, A. H. Wu and R. N. Lamb, *Acs Appl. Mater. Inter.*, 2014, **6**, 9503-9507.
19 X. Deng, L. Mammen, Y. Zhao, P. Lellig, K. Müllen, C. Li, H. J. Butt and D. Vollmer, *Adv. Mater.*, 2011, **23**, 2962-2965.
20 E. Huovinen, L. Takkunen, T. Korpela, M. Suvanto, T. T. Pakkanen and T. A. Pakkanen, *Langmuir*, 2014, **30**, 1435-1443.
21 A. M. Emelyanenko, F. M. Shagieva, A. G. Domantovsky and L. B. Boinovich, *Appl. Surf. Sci.*, 2015, **332**, 513-517.
22 H. Cho, D. Kim, C. Lee and W. Hwang, *Curr. Appl. Phys.*, 2013, **13**, 762-767.
23 B. G. Park, W. Lee, J. S. Kim and K. B. Lee, *Colloid.Surf. A: Physicochem. Eng. Asp.*, 2010, **370**, 15-19.
24 D. Ebert and B. Bhushan, *J. Colloid Interf. Sci.*, 2012, **368**, 584-591.
25 C. Su, Y. Xu, F. Gong, F. Wang and C. Li, *Soft Matter*, 2010, **6**, 6068-6071.
26 H. Zhou, H. Wang, H. Niu, A. Gestos, X. Wang and T. Lin, *Adv. Mater.*, 2012, **24**, 2409-2412.
27 Y. Li, L. Li and J. Sun, *Angew. Chem.*, 2010, **122**, 6265-6269.
28 C.-H. Xue, Z.-D. Zhang, J. Zhang and S.-T. Jia, *J. Mater. Chem. A*, 2014, **2**, 15001-15007.
29 N. Puretskiy, G. Stoychev, A. Synytska and L. Ionov, *Langmuir*, 2012, **28**, 3679-3682.
30 X. Zhu, Z. Zhang, X. Men, J. Yang, K. Wang, X. Xu, X. Zhou and Q. Xue, *J. Mater. Chem.*, 2011, **21**, 15793-15797.
31 A. Nakajima, K. Abe, K. Hashimoto and T. Watanabe, *Thin Solid Films*, 2000, **376**, 140-143.
32 J. Bravo, L. Zhai, Z. Wu, R. E. Cohen and M. F. Rubner, *Langmuir*, 2007, **23**, 7293-7298.
33 A. Cholewinski, J. Trinidad, B. McDonald and B. Zhao, *Surf. Coat. Technol.*, 2014, **254**, 230-237.
34 Y. Huang, M. Hu, S. Yi, X. Liu, H. Li, C. Huang, Y. Luo and Y. Li, *Thin Solid Films*, 2012, **520**, 5644-5651.
35 S. Ramakrishna, K. S. Kumar, D. Mathew and C. R. Nair, *J. Mater. Chem. A*, 2015, **3**, 1465-1475.
36 C. Wang, A. H. Wu and R. N. Lamb, *J. Phys. Chem. C*, 2014, **118**, 5328-5335.
37 H. Wang, J. Fang, T. Cheng, J. Ding, L. Qu, L. Dai, X. Wang and T. Lin, *Chem. Commun.*, 2008, 877-879.
38 H. Zhou, H. Wang, H. Niu, A. Gestos and T. Lin, *Adv. Funct. Mater.*, 2013, **23**, 1664-1670.
39 H. Ni, X. Wang, W. Zhang, X. Wang and Z. Shen, *Surf. Sci.*, 2007, **601**, 3632-3639.
40 T. Verho, C. Bower, P. Andrew, S. Franssila, O. Ikkala and R. H. Ras, *Adv. Mater.*, 2011, **23**, 673-678.
41 Y. Xiu, Y. Liu, D. W. Hess and C. Wong, *Nanotechnology*, 2010, **21**, 155705.
42 F. Su and K. Yao, *Acs Appl. Mater. Inter.*, 2014, **6**, 8762-8770.

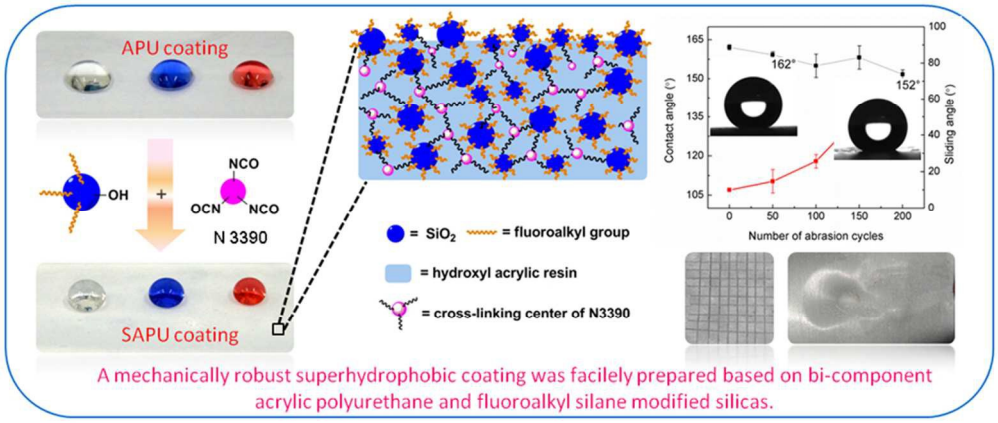

Graphical Abstract
80x33mm (300 x 300 DPI)